Int. J. Heat Mass Transfer. Vol. 15, pp. 2293–2308. Pergamon Press 1972. Printed in Great Britain

DEVELOPING LAMINAR FREE CONVECTION BETWEEN VERTICAL FLAT PLATES WITH ASYMMETRIC HEATING

W. AUNG

Bell Laboratories. Whippany. New Jersey. U.S.A.

and

L. S. FLETCHER and V. SERNAS

Department of Mechanical and Aerospace Engineering. Rutgers University. New Brunswick. New Jersey. U.S.A.

(*Received* 27 *September* 1971 *and in revised form* 18 *February* 1972)

Abstract—A numerical and experimental investigation of the developing laminar free convection heat transfer in vertical parallel plate channels with asymmetric heating is presented. Thermal boundary conditions of uniform wall heat fluxes (UHF) and uniform wall temperature (UWT) are considered. Solutions of the developing flow are obtained for air at different ratios of the wall heat fluxes and wall temperature differences (above the temperature of the fluid at the channel entrance). The numerical solutions are shown to approach asymptotically the closed form solution for fully developed flow. The present results indicate that for UHF. the difference between the maximum temperatures on the two walls diminishes as fully developed flow is achieved. For UWT. the Nusselt number characterizing the total heat transfer to the fluid is found to be related to the Rayleigh number very nearly by a universal curve for all ratios of wall temperature differences, providing the Nusselt and Rayleigh numbers are appropriately defined.

NOMENCLATURE

b, channel width;

c, specific heat of fluid;

g, gravitational acceleration;

k, thermal conductivity of fluid;

l, channel height;

p, fluid pressure;

p_0, hydrostatic fluid pressure;

Pr, Prandtl number defined by equation (4a);

q, heat flow from wall per unit area per unit time;

Q'_L, heat absorbed by fluid between channel entrance and channel exit,

$$\rho c\left[\int_0^b u(T - T_0)\,dy\right]_{x=l};$$

r_H, r_T, ratio of wall heat fluxes or wall temperature differences defined by equation (5);

T, fluid temperature;

T_0, temperature of fluid at channel entrance;

ΔT, $T - T_0$;

u, fluid velocity in x-direction;

u_0, average fluid velocity;

UHF, uniform wall heat fluxes;

UWT, uniform wall temperatures;

v, fluid velocity in y-direction;

x, y, rectangular coordinate system, see Fig. 1(b);

β, thermal expansion coefficient of fluid;

μ, dynamic viscosity of fluid;

ν, kinematic viscosity of fluid;

ρ, density of fluid;

θ, dimensionless temperature defined by equations (4b) or (4c);

Subscripts

1, refers to hotter wall;
2, refers to cooler wall;
$\frac{1}{2}$, value or based on value at mid-height of channel;
max, maximum value;
w, wall value;
x, value at distance x from channel entrance.

A bar over a symbol indicates definition using the average of the wall temperatures or the average of the wall heat fluxes.

INTRODUCTION

SEVERAL investigators have studied laminar free convection in vertical, parallel-plate channels. All of them, however, have restricted their consideration to either identical heating of the two walls [1–4] or the so-called "fully developed" flow that characterizes a channel whose height is large compared to the spacing between the walls [4–7]. The majority of the latter studies [5–7] deal with combined free and forced convection. In the case of vertical tubes, to the present authors' knowledge, all published free convection results, for example [8], have been for symmetrically heated tubes. The effect of asymmetric heating in free convection, therefore, has not been fully investigated, although the corresponding problem in forced convection has been quite extensively studied. References for the latter case are not relevant to the present study and hence will not be listed here.

The present study concerns a theoretical and experimental investigation of the laminar free convection in air in a parallel-plate vertical flat duct. The duct walls are individually heated uniformly or maintained at constant temperatures. The wall heat fluxes or wall temperatures, however, need not be the same. Practical application of free convection in vertical channels with asymmetric heating of this nature may be found in modern communication equipment. In such equipment, vertical circuit cards containing heat generating electronic devices are arrayed to form vertical channels, and are cooled by free convection.

THEORETICAL ANALYSIS

Governing equations

The flow geometry of interest is depicted in Fig. 1(a) which shows a vertical flat duct of height l and width b. The channel walls are heated and as a result of the heat transfer to the fluid, the temperature of the latter increases. The resultant density differences cause the fluid to rise. The fluid that enters the channel from the bottom at the temperature T_0 is assumed to have a flat velocity profile u_0.

The dimensionless equations expressing the conservation of mass, momentum and energy for laminar, constant property (except for density difference in the buoyancy term) boundary layer flows are (see [2]):

$$\frac{\partial U}{\partial X} + \frac{\partial V}{\partial Y} = 0 \tag{1}$$

$$U\frac{\partial U}{\partial X} + V\frac{\partial U}{\partial Y} = \frac{\partial^2 U}{\partial Y^2} - \frac{\mathrm{d}P}{\mathrm{d}X} + \theta \tag{2}$$

$$U\frac{\partial \theta}{\partial X} + V\frac{\partial \theta}{\partial Y} = \frac{1}{Pr}\frac{\partial^2 \theta}{\partial Y^2} \tag{3}$$

where

$$\left.\begin{aligned} U &= \frac{b^2 u}{lvGr},\ V = \frac{bv}{v},\ X = \frac{x}{lGr},\ Y = \frac{y}{b} \\ P &= \frac{(p - p_0)b^4}{\rho l^2 v^2 Gr^2},\quad Pr = \frac{\mu c}{k}. \end{aligned}\right\} \tag{4a}$$

Note that p_0 is the pressure that would apply at any level in the channel if the fluid therein were at the ambient temperature T_0. For uniform wall heat fluxes,

$$\theta = \frac{T - T_0}{q_1 b/k},\ Gr = \frac{g\beta q_1 b^5}{lv^2 k}\ (\mathrm{UHF}). \tag{4b}$$

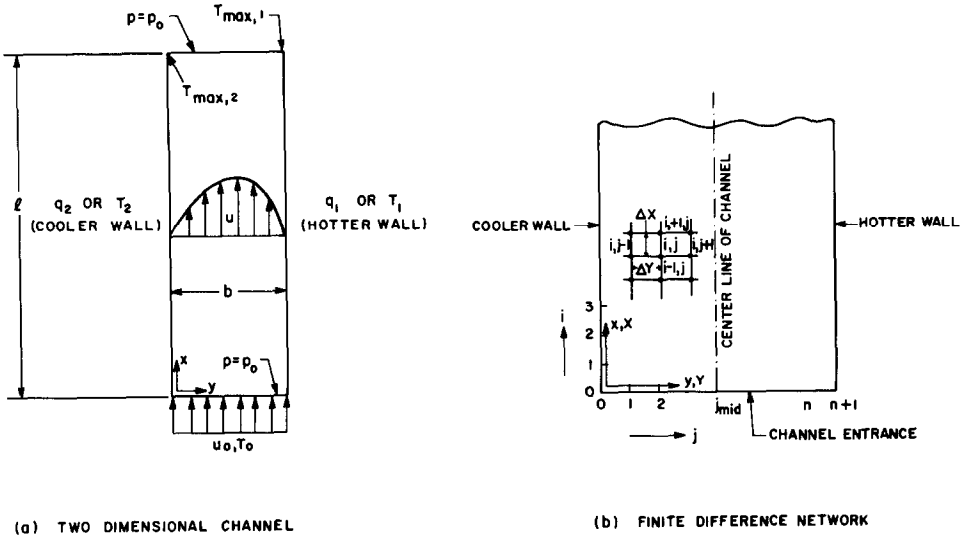

FIG. 1. Model of analysis.

For uniform wall temperatures,

$$\theta = \frac{T - T_0}{T_1 - T_0}, \; Gr = \frac{g\beta(T_1 - T_0)\, b^4}{lv^2} \text{ (UWT)}. \tag{4c}$$

Denoting the heat flux on the cooler wall by q_2 and the cooler wall temperature by T_2, we write the heat flux and temperature difference ratios

$$r_H = \frac{q_2}{q_1}, \; r_T = \frac{T_2 - T_0}{T_1 - T_0} \tag{5}$$

where r_H and r_T vary from 0 to 1. The boundary conditions can be expressed as:

for $X = 0$ and $0 < Y < 1$:

$$U = M, \; V = 0, \; \theta = 0$$

for $Y = 0$ and $X \geqslant 0$:

Uniform Heat Fluxes:

$$U = 0, \quad V = 0, \; \frac{\partial \theta}{\partial Y} = -r_H$$

Uniform Wall Temperatures:

$$U = 0, \quad V = 0, \; \theta = r_T$$

for $Y = 1$ and $X \geqslant 0$:

Uniform Heat Fluxes:

$$U = 0, \; V = 0, \; \frac{\partial \theta}{\partial Y} = 1$$

Uniform Wall Temperatures:

$$U = 0, \quad V = 0, \; \theta = 1$$

at $X = 0$ and $X = L$;

$$P = 0,$$

(6)

where the dimensionless flow rate is given by

$$M = \frac{u_0 b^2}{lvGr} = \int_0^1 U \, dY. \tag{7}$$

The dimensionless channel length L is the value of X when $x = l$, that is

$$L = \frac{1}{Gr}. \tag{8}$$

The average of the wall heat fluxes and the average of the wall temperature differences are:

$$\bar{q} = \tfrac{1}{2}(q_1 + q_2) = q_1\left(\frac{1 + r_H}{2}\right)$$

$$\overline{\Delta T_T}\quad T_0 = \tfrac{1}{2}[(T_1 - T_0) + (T_2 - T_0)]$$

$$= (T_1 - T_0)\left(\frac{1 + r_T}{2}\right). \tag{9a}$$

For either UHF or UWT, the dimensionless parameters of the problem may be alternately defined using the appropriate average quantity given above. The relation between some of these redefined parameters and the corresponding ones used so far are:

$$\left.\begin{aligned} \overline{M} = M\left(\frac{2}{1 + r}\right);\ \overline{P} = P\left(\frac{2}{1 + r}\right)^2;\\ \overline{Gr} = Gr\left(\frac{1 + r}{2}\right);\\ \overline{X} = X\left(\frac{2}{1 + r}\right);\ \overline{L} = L\left(\frac{2}{1 + r}\right);\\ \bar{\theta} = \theta\left(\frac{2}{1 + r}\right) \end{aligned}\right\} \tag{9b}$$

where r can be either r_H or r_T.

Fully developed flow

Fully developed flow is closely approached in a channel whose length is large compared with its width, that is, when L is large. The study of this flow is, therefore, useful; it is also instructive because it yields the limiting conditions for the developing flow. Solutions for fully developed flow may be acquired in closed forms and are indicated in [9]. In this paper it will be shown that the fully developed flow results are asymptotically approached by the numerically obtained solutions for developing flow.

Finite difference solution for developing flow

The solution of the governing equations for developing flow is discussed in this section. Considering the finite difference grid network of Fig. 1(b), equations (2) and (3) are replaced by by the following difference equations which were also used in [2].

$$U_{i,j}\frac{U_{i+1,j} - U_{i,j}}{\Delta X} + V_{i,j}\frac{U_{i+1,j+1} - U_{i+1,j-1}}{2\Delta Y} = \frac{U_{i+1,j+1} - 2U_{i+1,j} + U_{i+1,j-1}}{(\Delta Y)^2} - \frac{P_{i+1} - P_i}{\Delta X} + \theta_{i+1,j} \tag{10}$$

$$U_{i,j}\frac{\theta_{i+1,j} - \theta_{i,j}}{\Delta X} + V_{i,j}\frac{\theta_{i+1,j+1} - \theta_{i+1,j-1}}{2\Delta Y} = \frac{1}{Pr}\frac{\theta_{i+1,j+1} - 2\theta_{i+1,j} + \theta_{i+1,j-1}}{(\Delta Y)^2}. \tag{11}$$

To calculate V, the transverse component of velocity, the centerline value of the index is denoted (see Fig. 1(b))

$$j_{\text{mid}} = \frac{n + 3}{2}$$

where $n + 2$ is the total number of nodes along Y and is an odd integer. For $j < j_{\text{mid}}$ the continuity equation (1) can be written

$$V_{i+1,j} = V_{i+1,j-1} - \frac{\Delta Y}{2\Delta X}(U_{i+1,j} + Y_{i+1,j-1} - U_{i,j} - U_{i,j-1}),\ j = 1, 2, 3, \ldots, j_{\text{mid}} - 1. \tag{12a}$$

For $j > j_{\text{mid}}$, the above equation is modified and the following form is used:

$$V_{i+1,j} = V_{i+1,j+1} + \frac{\Delta Y}{2\Delta X}(U_{i+1,j} + U_{i+1,j+1} - U_{i,j} - U_{i,j+1}),$$
$$j = n, n - 1, n - 2, \ldots, j_{\text{mid}} + 1. \tag{12b}$$

In principle, either of equation (12a) and equation (12b) could be used to evaluate the centerline velocity $V_{i+1,j_{mid}}$. However, since both equations employ one-sided differences, a different value of $V_{i+1,j_{mid}}$ could result depending on which equation is considered. Consequently, the transverse velocity at the centerline is calculated by fitting a third order polynomial through the values on the two immediate mesh points on both sides of the centerline.

By means of Simpson's rule, we write equation (7) as

$$4U_{i+1,1} + 2U_{i+1,2} + 4U_{i+1,3} + 2U_{i+1,4} + \cdots + 4U_{i+1,n} = (n+1)M. \quad (13)$$

The solution of the difference equations is obtained by first selecting values for Pr, M and r_H or r_T. Then by means of a marching procedure the variables U, V, θ and P for each row beginning at row $i+1=2$ are obtained using the values at the previous row i. Thus by applying equations (10), (11) and (13) to the points $1, 2, 3, \ldots, n$ on row i, $2n+1$ algebraic equations with the $2n+1$ unknowns $U_{i+1,1}, U_{i+1,2}, \ldots, U_{i+1,n}$, $P_{i+1}, \theta_{i+1,1}, \theta_{i+1,2}, \ldots, \theta_{i+1,n}$ are obtained. This system of equations is then solved by a matrix reduction technique. Equations (12) are then used to calculate $V_{i+1,1}, V_{i+1,2}, \ldots, V_{i+1,n}$. The procedure is continued until the pressure P returns to zero or becomes positive at which point the solution is terminated. This determines L for input M. If $P > 0$ at termination then L is evaluated at $P = 0$ by linear interpolation.

Typically 41 meshpoints are used in the Y-direction at the channel entrance and this number is reduced as X increases. (Use of 81 meshpoints in the Y-direction at the channel entrance does not significantly alter the results.) A progressively larger step size is also used in the X-direction, beginning with an axial step size at the channel entrance, as it turns out in all cases, of about 0·1 per cent of the channel height. In some cases, the effect of the axial step size is checked by re-running the solutions after increasing the step sizes by a factor or two. No significant effect on the calculated local distribution of the variable of interest or of the computed channel height is noticed.

Note that for the condition of uniform wall temperatures, the boundary temperatures $\theta_{i+1,0}$ and $\theta_{i+1,n+1}$ are specified. In the case of uniform heat fluxes, the wall temperatures gradients are specified instead of the wall temperatures. Hence the solutions for UHF are obtained by successive approximations as follows. For any row $i+1$, we first set the wall temperatures equal to those on the previous row, that is (employing "primes" to designate successive approximates)

$$\theta'_{i+1,0} = \theta_{i,0}, \quad \theta'_{i+1,n+1} = \theta_{i,n+1}.$$

Using these a solution for the interior points at row $i+1$ is obtained as described above. Then by means of a three-point derivative formula, new wall temperatures are computed by setting

$$\theta''_{i+1,0} = (4\theta'_{i+1,1} - \theta'_{i+1,2} + 2r_H\Delta Y)/3$$

$$\theta''_{i+1,n+1} = (4\theta'_{i+1,n} - \theta'_{i+1,n-1} + 2\Delta Y)/3.$$

With these, a new solution for the interior points at row $i+1$ may be obtained. The procedure is continued until, for some successive approximates θ^N and θ^{N+1} of the wall temperatures, the condition $(\theta^{N+1} - \theta^N)/\theta^{N+1} \leqslant \varepsilon$, where ε is an arbitrary small number, holds true simultaneously for both wall temperatures. Values of 0·01 and 0·001 have been used for ε without significant differences in the results. Consequently, the value $\varepsilon = 0{\cdot}001$ is used.

EXPERIMENTAL METHODS

Experiments were conducted to verify the theoretical results. The boundary conditions used were constant wall temperatures. A channel with isothermal walls of different temperatures was made from aluminium plates 7 in. by 7 in. in size and 0·5 in. thick. The hotter plate was heated by a heated water pool and the colder plate was heated by circulating a warm water–

oil mixture through a maze of grooves machined into the back of the plate. Glass plates of optical quality and 0·5 in. thickness were clamped and sealed on the vertical edges of the two isothermal plates to complete the channel geometry.

While the temperatures of the isothermal walls were maintained at 205°F and 126°F, heat transfer tests were run for six different channel widths varying from 0·188 in. to 0·75 in. The temperature over each plate was monitored by twelve thermocouples imbedded near the channel surface throughout the two plates. The thermocouples indicated that each plate never varied in temperature more than $\pm 0{\cdot}02$°F. The channel spacing was measured with a precision dial indicator that was zeroed when the two isothermal plates were made to touch each other. As the two plates were separated by a rack and pinion slide to form a channel, the indicator dial was read directly for the channel width. It was estimated that the recorded channel width could not have been in error by more than $\pm 0{\cdot}002$ in.

In each test, the heat flux from each wall of the channel was measured interferometrically with a Wollaston prism schlieren interferometer. Details of the interferometer including the method of data evaluation are contained in [10–12].

The temperature field in the fluid was also studied qualitatively by means of a holographic interferometer. This instrument is described in [13]. The test section used in these measurements was similar to the one described above, except that the aluminium plates were 15 in. high, 10 in. wide, $\frac{1}{4}$ in. thick and were heated individually by passing a.c. currents through nichrome wires imbedded in the plates. Using a constant temperature hot wire anemometer and a thermocouple probe, velocity and temperature traverses were also made near the channel exit. The anemometer was a Thermo-Systems Inc. Model 1050 used in conjunction with a Model 1060 RMS voltmeter and a 1150 calibrator. A more elaborate calibration procedure for low velocity measurements, such as described in [14], was not carried out. Nevertheless, inasmuch as the objective was to obtain a quick check of the theoretical solutions, the present method was considered adequate.

RESULTS

Results are obtained from the numerical solution for air ($Pr = 0{\cdot}7$) for both the condition of uniform wall heat fluxes and uniform wall temperatures. The solution for these two conditions are discussed individually in the following.

(i) *Uniform wall heat fluxes*

For the vertical channel whose walls are heated uniformly, solutions are obtained for heat flux ratios of 0 (corresponding to the condition in which the cooler wall is insulated), 0·1, 0·5 and 1 (representing symmetric heating of the two walls). The relation between the dimensionless mass flux $\bar{M}$ and the dimensionless channel length $\bar{L}$ is plotted in Fig. 2. When $\bar{L} \geqslant 10^{-2}$, the curves for different values of r_H are indistinguishable from each other and coincide with the fully developed flow asymptotic solutions.

Computed temperature and velocity profiles from the numerical solution for $r_H = 0$ at $\bar{M} = 0{\cdot}15$ and $0{\cdot}005$ are indicated in Fig. 3. The colder wall is represented by the line $Y = 0$. The profiles for the larger value of $\bar{M}$ change little in shape throughout the entire channel. At the smaller value of $\bar{M}$ (Fig. 3b), the specified uniform velocity at $X = 0$ is seen transformed near the channel exit into one indicating higher flow velocities adjacent to the hotter wall. Physically this type of profile, which is akin to that about a single vertical plate in free convection, is the more realistic one when $\bar{L}$ (and hence $\bar{M}$) is small (for example, when the channel width b is large so that the channel walls are thermally independent of one another) and should exist in the entire channel. The specification of a uniform entrance velocity distribution is, therefore, incorrect and its

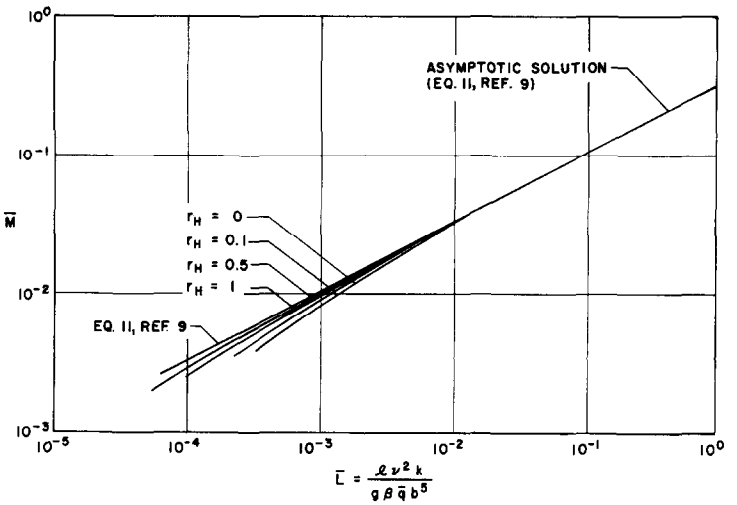

FIG. 2. Relation between volume flow rate and channel length for UHF.

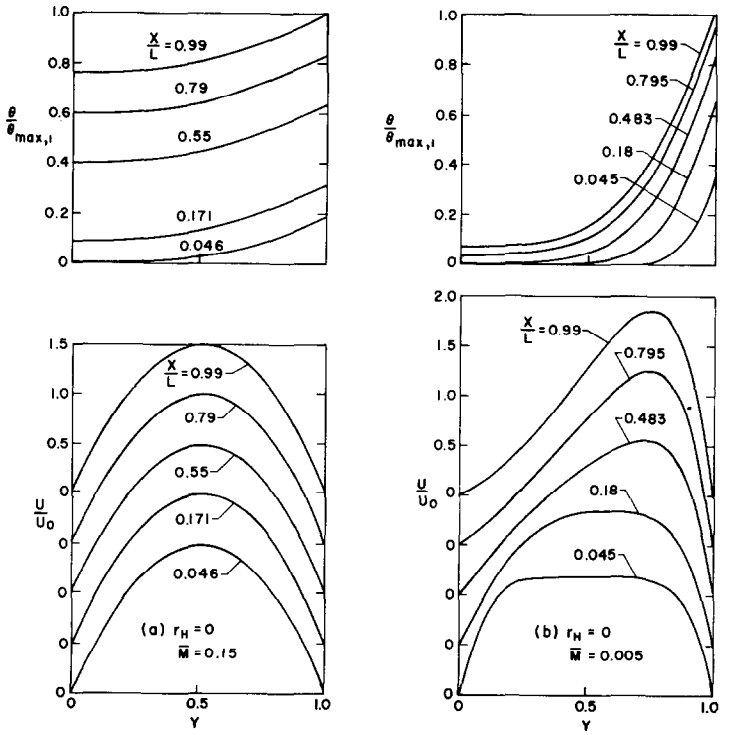

FIG. 3. Calculated velocity and temperature fields from numerical solutions for UHF.

significance on the heat transfer will be discussed later.

Numerically computed axial pressure variation is plotted in Fig. 4(a) for $\bar{M} = 0{\cdot}15$. The pressure distribution for all values of r_H is represented closely by the single curve shown. This curve is higher than that for fully developed flow which is also plotted. The trend remains unchanged for larger values of $\bar{M}$ but, when $\bar{M}$ is larger, the agreement between the numerical solution and the fully developed flow solution

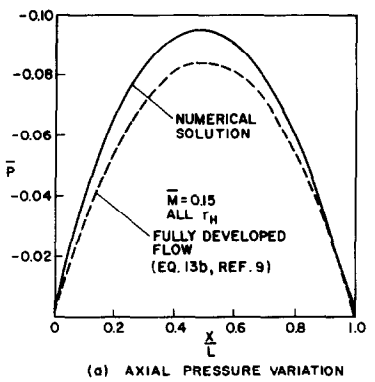

(a) AXIAL PRESSURE VARIATION

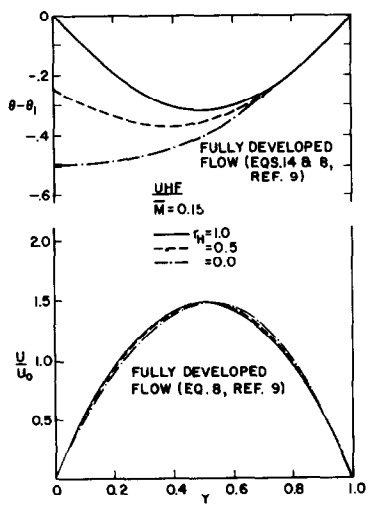

(b) TRANSVERSE TEMPERATURE AND VELOCITY DISTRIBUTIONS

FIG. 4. Fully developed flow axial pressure variation and transverse temperature and velocity distributions for UHF at $\bar{M} = 0{\cdot}15$.

becomes closer. This can be expected since the fully developed result is strictly valid only when $\bar{L} \to \infty$ (and hence $\bar{M} \to \infty$).

Velocity and temperature profiles at the channel exit from the numerical solution for $\bar{M} = 0{\cdot}15$ agree excellently with the fully developed flow distributions. This is not surprising since for $\bar{M} = 0{\cdot}15$, the conditions of fully developed flow are approached near the channel exit, as exhibited by the linear variation of the wall temperature which will be discussed later. The fully developed flow profiles are plotted in Fig. 4(b) for $r_H = 1{\cdot}0$, $0{\cdot}5$ and $0{\cdot}0$. While the velocity distribution for symmetric heating is similar to the Poiseuille flow profile, the fully developed profiles for asymmetric heating are seen to be slightly skewed, so that a larger quantity of fluid flows in the half-channel adjacent to the hotter wall (on the right in the figure).

The maximum temperatures on the two walls occur at the channel exit, and are plotted in Fig. 5 in dimensionless forms against the parameter $\bar{L}$. This figure indicates that at all values of r_H, the difference between the magnitudes of the maximum temperatures on the two channel walls diminishes as $\bar{L}$ increases. At $\bar{L} \geqslant 5$, the maximum temperature on the hotter wall ($\bar{\theta}_{\max,1}$) may be calculated with good accuracy by the fully developed flow solution. In the same range of $\bar{L}$, the fully developed flow result gives the maximum temperature on the cooler wall ($\bar{\theta}_{\max,2}$) to within a 6 per cent accuracy. At $\bar{L} \to \infty$, the maximum temperatures on the two walls become identical and the fully developed flow solution then exactly gives the magnitudes of these temperatures.

The results represented by the solid curves (hotter plate) in Fig. 5 are rephrased and plotted in terms of the variables $\theta_{\max,1}$ and L in Fig. 6. In this manner the solution for $r_H = 1$ may be compared with those obtained in [3] by an integral technique. The agreement is seen to be good. The dashed line in Fig. 6 represents the single plate solution of [15] for $Pr = 0{\cdot}7$, with minor variable transformations. It is

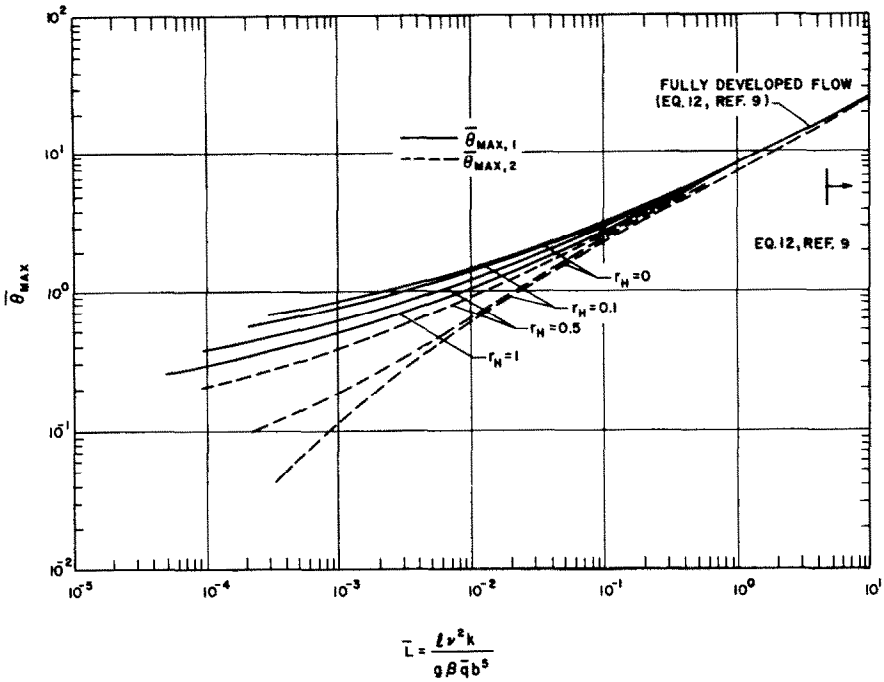

FIG. 5. Relation between dimensionless maximum wall temperature and dimensionless channel length of UHF.

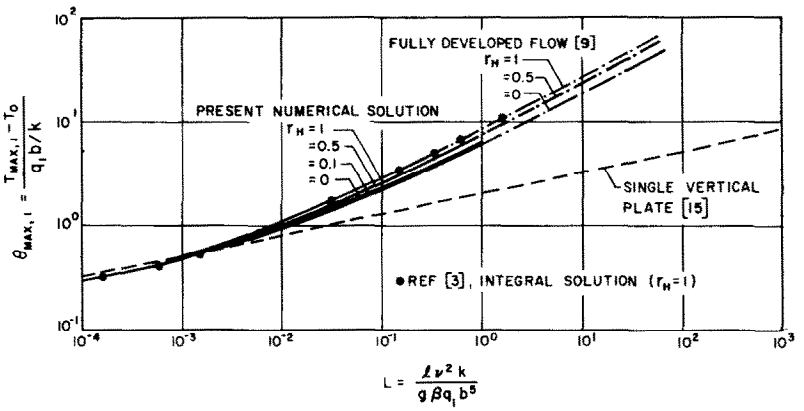

FIG. 6. Comparison of maximum hot wall temperatures with the results of Engel and Mueller [3] and Sparrow and Gregg [15] for UHF.

noted that the result for a single vertical plate may be applied when $L \leqslant 10^{-3}$. This condition is also approximately valid for the cooler plate. Note that in this range the present solution predicts a smaller (by about 10 per cent) maximum wall temperature than the single plate solution does, as is apparent from Fig. 6. This discrepancy is believed to be caused by the assumption in the present numerical solution of a uniform velocity profile at the channel entrance. This assumption is not realistic when $\bar{L}$ or L is small, as noted previously. Similar

difficulty was encountered by Bodoia and Osterle [2] for UWT at $r_T = 1$ using the same assumption, giving rise in that case to a larger heat transfer from the channel walls when compared to the corresponding single plate solution.

Typical spatial variation of the local wall temperatures are plotted in Fig. 7 for $\bar{M} = 0{\cdot}005$ and $\bar{M} = 0{\cdot}15$. The behavior of the

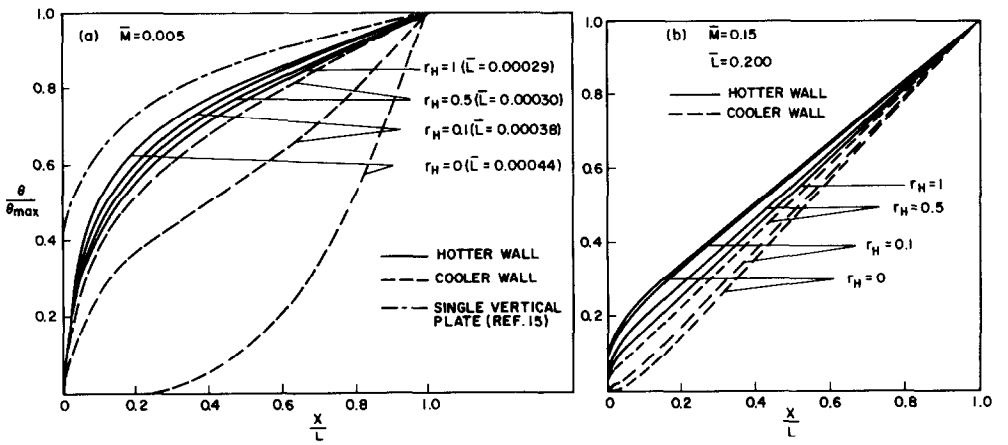

FIG. 7. Typical axial variations of the wall temperatures at small and large $\bar{M}$ for UHF.

temperature on the hotter wall for the smaller $\bar{M}$ is similar to that on a single vertical flat plate [15] which is also shown. At the higher value of $\bar{M}$, the variation of wall temperature is linear (fully developed) with axial distance for both walls over a considerable portion of the channel.

The curves given in Fig. 7 may also be employed to evaluate local heat transfer coefficients, which may be useful in design calculations. The reason is that the dimensionless local temperature θ is related to the local Nusselt numbers as follows:

$$Nu_{x,1} = \frac{h_{x,1}b}{k} = \frac{q_1}{(T_{x,1} - T_0)} \cdot \frac{b}{k} = \frac{1}{\theta_{x,1}},$$

$$Nu_{x,2} = \frac{h_{x,2}b}{k} = \frac{q_2}{(T_{x,2} - T_0)} \cdot \frac{b}{k} = \frac{r_H}{\theta_{x,2}}.$$

Similarly, an average Nusselt number characterizing the heat transfer to the fluid in the entire channel may be defined using the maximum temperature on the channel wall and Fig. 5 may be used to evaluate this Nusselt number. Alternatively, an average Nusselt number $\overline{Nu}_{\frac{1}{2}}$ may be formed using the average of the two wall temperatures at mid-height. This definition is an extension of that for a single, uniformly heated vertical plate [15]. (For a channel whose height (l) is large compared with its width (b), the mid-height temperature on each wall is very close to the average temperature on the entire wall.) Thus, in the present case,

$$\overline{Nu}_{\frac{1}{2}} = \frac{\bar{q}b}{(\bar{T}_{\frac{1}{2}} - T_0)k} = \frac{2}{\bar{\theta}_{\frac{1}{2},1} + \bar{\theta}_{\frac{1}{2},2}}.$$

In Fig. 8, $\overline{Nu}_{\frac{1}{2}}$ is plotted against the Rayleigh number $\overline{Ra}$ where

$$\overline{Ra} = Pr \times \overline{Gr} = Pr/\bar{L}.$$

For all heat flux ratios the results are represented very closely by the single curve shown. This curve is seen to agree with the results of [3] for symmetric heating.

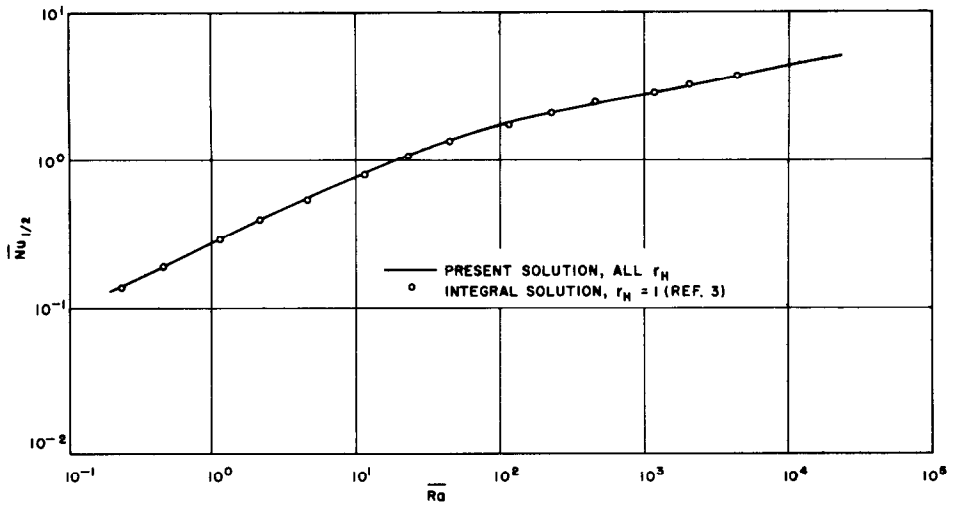

FIG. 8. Average Nusselt number as a function of Rayleigh number for UHF.

Uniform wall temperature

Consideration is now given to the case of UWT. Numerical solutions for the developing flow are obtained for wall temperature difference (above the temperature of the entering fluid) ratios of 1, 0·5, 0·1 and 0, where $r_T = 1$ corresponds to symmetric heating of the two walls. The case $r_T = 1$ has been considered by Bodoia and Osterle [2].

The relation between $\bar{M}$ and $\bar{L}$ is shown in Fig. 9. In contrast to UHF, at large values of $\bar{L}$ the mass flow parameter $\bar{M}$ for UWT approaches an asymptotic value of 1/12. The latter is the fully developed flow value [9]. Calculated temperature and velocity profiles from the numerical solution for $\bar{M} = 0{\cdot}8$ agree with the profiles for fully developed flow ($\bar{M} = \frac{1}{12}$). The fully developed profiles [9] are

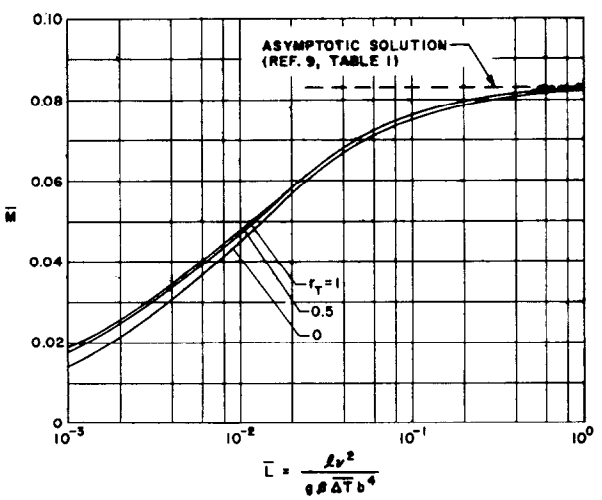

FIG. 9. Relation between dimensionless volume flow rate and dimensionless channel length for UWT.

plotted in Fig. 10. One of the cases plotted ($r_T = 0.5$) was compared to a similar case considered in [5]. Very close agreement was discovered. Also shown in Fig. 10 are some experimental measurements taken at the channel exit by means of hot wire anemometry and thermocouple traverses. The measurements are seen to agree reasonably

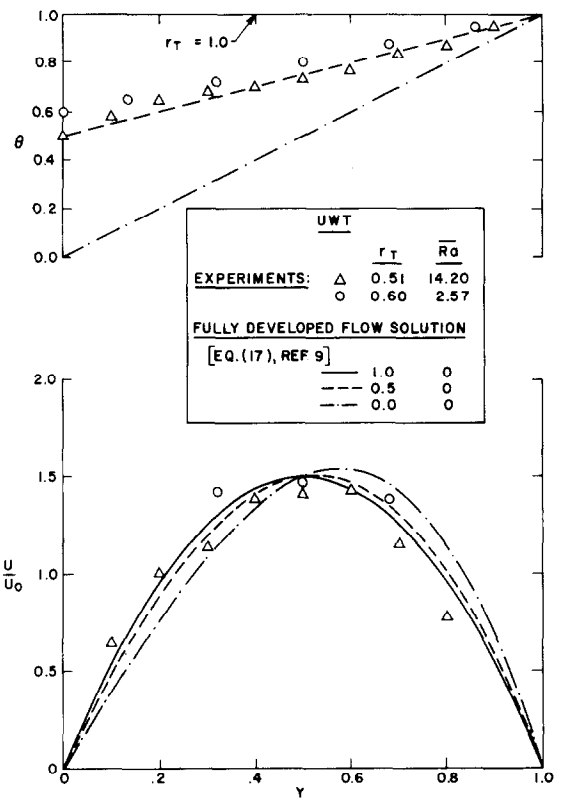

FIG. 10. Fully developed flow temperature and velocity distributions for UWT and comparison with measurements.

well with the theoretical result. The scatter of the data is attributable to flow fluctuations near the channel exit due to the presence of minor room air currents.

The local heat transfer coefficient may be defined based on the temperature of the hotter wall, that is

$$(h_x)_i = -\frac{k}{(T_1 - T_0)}\left(\frac{\partial T}{\partial y}\right)_i, i = 1,2,$$

where $i = 1$ refers to the hotter wall and $i = 2$ cooler wall. With this, the local Nusselt number may be defined

$$(Nu_x)_i = \frac{(h_x)_i b}{k} = -\left(\frac{\partial \theta}{\partial Y}\right)_i, i = 1,2.$$

Calculated local Nusselt numbers are plotted in Fig. 11(a) for $\overline{M} = 0.08$. It is clear that, along a large extent of the channel (fully developed flow region), the heat transfer at the two walls is equal and opposite in direction and the net heat transfer to the fluid is zero.

Figure 11(b) shows the local Nusselt numbers from the numerical solution for a special case which matches the experimental conditions in one test in which $\overline{Ra} = 24$, $r_T = 0.33$, where the Rayleigh number $\overline{Ra}$ is defined as

$$\overline{Ra} = Pr \times \overline{Gr}.$$

The experimental data are obtained using the schlieren interferometer. Good agreement between the theoretical and experimental results may be noted, except at $X/L \lesssim 0.1$ on the hotter wall. Near the leading edge of the hotter plate, it is believed that the temperature was slightly lower due to the construction of the apparatus, thereby resulting in a lower heat flux. The corresponding Schlieren interferogram from which the experimental data are taken is shown in Fig. 12.

An average Nusselt number is defined using the net heat transfer and the average of the wall temperature differences, that is:

$$\overline{Nu} = \frac{Q'_L b}{2l(\overline{T} - T_0)k}.$$

It is plotted in Fig. 13 against the Rayleigh number $\overline{Ra}$. The numerical solutions for all wall temperature difference ratios differ very little from one another over the range of $\overline{Ra}$ investigated, so that only the results for $r_T = 0$ and $r_T = 1$ are plotted. The curve for $r_T = 1$ coincides with the solutions of Bodoia and

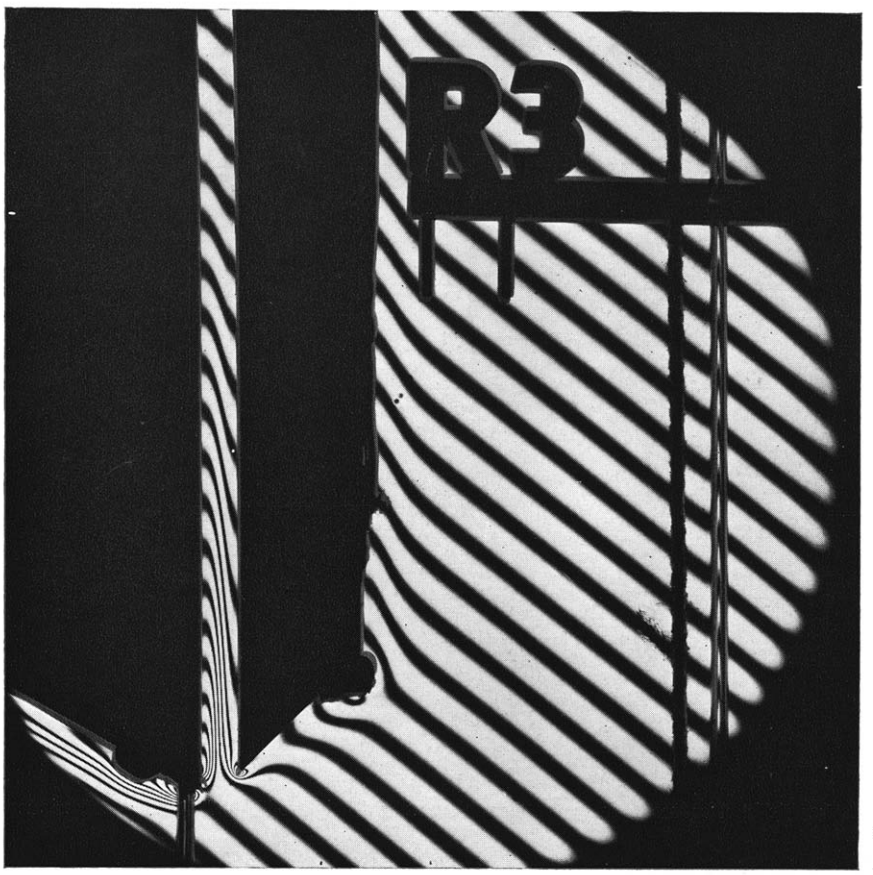

FIG. 12. Schlieren interferometer fringe pattern in UWT channel corresponding to data shown in Fig. 11(b).

[*facing page* 2304]

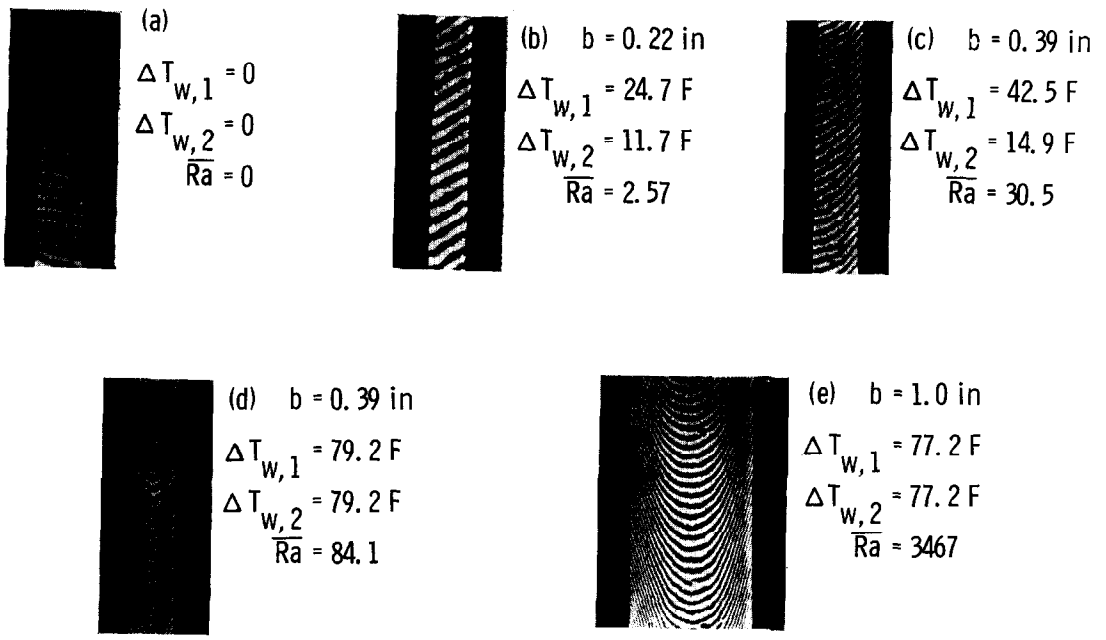

FIG. 14. Holographic interferometer fringe pattern taken at mid-height of UWT channel for various values of $\overline{Ra}$.

Osterle [2] which are not indicated in the figure. For $\overline{Ra} \leqslant 2$ the present numerical results are indistinguishable from the fully developed results [9].

Also indicated in Fig. 13 are experimental data from schlieren interferometry as well as from velocity and temperature traverses in the fluid at the channel exit. From the schlieren interferometer data, the net heat transfer to the fluid is obtained by graphical integration of the local heat flux distribution. From the velocity and temperature traverses, it is acquired

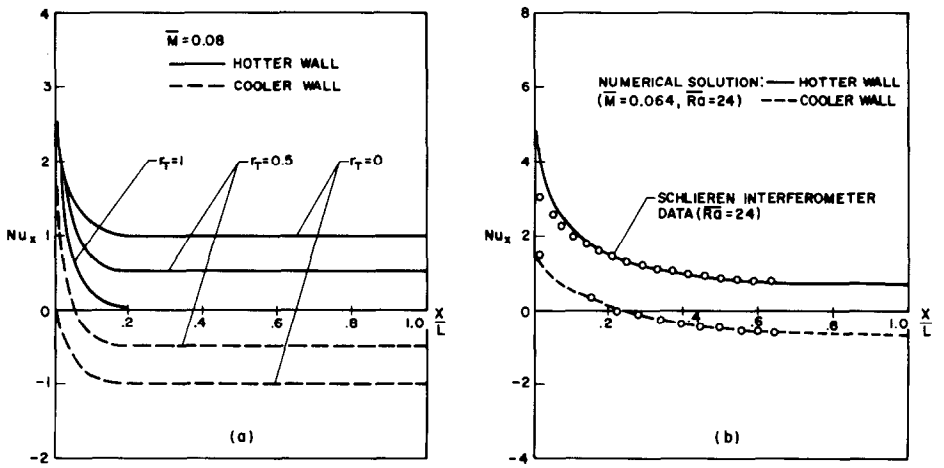

FIG. 11. Local Nusselt number for UWT based on temperature difference on hotter wall and comparison with measurements.

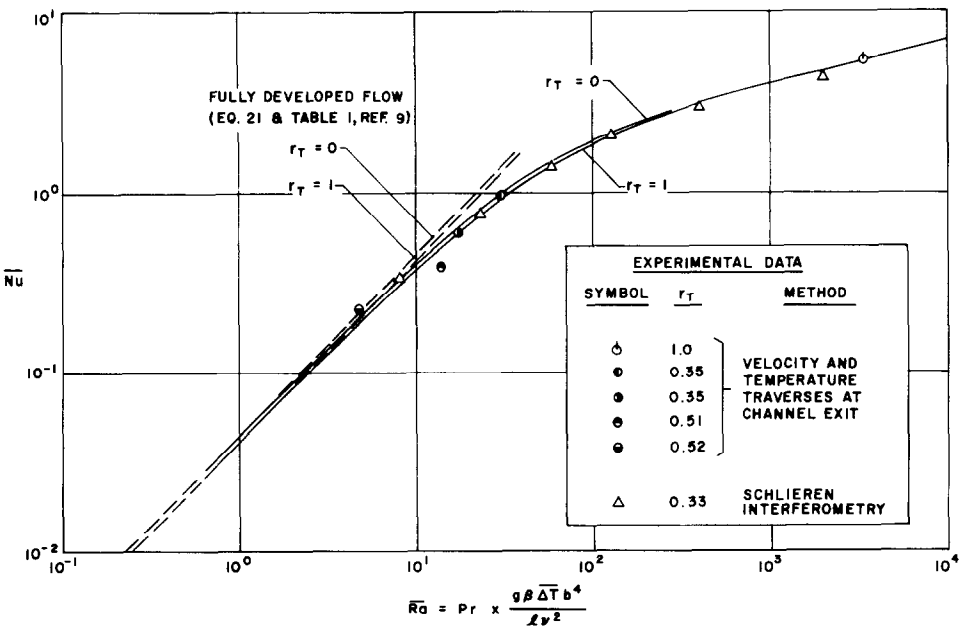

FIG. 13. Average Nusselt number as a function of Rayleigh number for UWT and comparison with measurements ($\overline{Nu}$ and $\overline{Ra}$ are based on $\overline{\Delta T}$).

by evaluating Q'_L. Fluid properties are evaluated at a temperature which is $(\overline{T} + T_0)/2$ where $\overline{T}$ is the average of the wall temperatures.

The experimental data in Fig. 13 exhibit some scatter. However, the schlieren data, which are the more accurate ones, generally agree with the theoretical results although at $\overline{Ra} > 400$ these experimental data tend to be lower (by about 10 per cent) than the theoretical solutions. In this range of $\overline{Ra}$, Bodoia and Osterle's [2] numerical solutions for $r_T = 1$ are also higher than the experimental data of Elenbaas [1] by about 10 per cent and these authors ascribe the discrepancies to the assumption of a flat velocity profile at the channel entrance.

Finally, Fig. 14 shows the interferometric ("finite fringe") patterns taken in the vicinity of the mid-height of the channel. These interferograms are intended for a qualitative study of the temperature field in the fluid at different test conditions. Real-time holographic interferometry is employed. Each fringe in the figure essentially represents the temperature variation in the fluid. The temperature distribution is seen to progressively deviate from a linear profile with successive increase in the Rayleigh number. With the aid of Fig. 13, it is possible to trace the evolution of the temperature profile from that typical of fully developed flow (at small $\overline{Ra}$) to that characteristic of laminar boundary layer flow (at large $\overline{Ra}$).

CONCLUSIONS

The effects of asymmetric heating on the free convection heat transfer in parallel plate vertical channels in air have been investigated in this study. Two thermal conditions of the channel walls are considered: uniform heat fluxes and uniform wall temperatures. Numerical solutions are obtained for the developing flow and are shown to asymptotically approach the closed form solutions for fully developed flow. In the case of uniform wall temperatures, the validity of the theoretical results is verified by experimental measurements.

When the channel walls are heated uniformly, it is found that when $\bar{L} \geqslant 5$, the maximum temperature on the two walls differ by less than 6 per cent from each other for all ratios of the wall heat fluxes. In this case, the fully developed flow solutions may be used to obtain these temperatures. When $L \leqslant 10^{-3}$ the present numerical solutions underpredict the maximum temperature on the hotter wall by 10 per cent when compared to the single plate solution.

For uniform wall temperatures, the present solutions give the average Nusselt number which describes the heat transfer to the fluid. The average Nusselt number is found to be related to the Rayleigh number very nearly by a universal curve for all wall temperature difference ratios, providing the average of the two wall temperature differences (above the temperature of the fluid at the channel entrance) is used to define these parameters. When this Rayleigh number is less than 2, the average Nusselt number is accurately given by the explicit expressions from the fully developed flow solution. When the Rayleigh number is greater than about 400, the present numerical solutions over-predict the average Nusselt number by about 10 per cent.

ACKNOWLEDGEMENTS

Acknowledgements are due from one of the authors (WA) to Dr. R. J. Prutow and Mr. A. J. Colucci of Bell Laboratories for helpful discussions and valuable aid in acquiring some of the experimental results.

REFERENCES

1. W. ELENBAAS. Heat dissipation of parallel plates by free convection. *Physica* **9**. 1–28 (1942).
2. J. R. BODOIA and J. F. OSTERLE. The development of free convection between heated vertical plates. *J. Heat Transfer* **84**. 40–44 (1962).
3. R. K. ENGEL and W. K. MUELLER. An analytical investigation of natural convection in vertical channels. ASME Paper No. 67-HT-16 (1967).
4. S. OSTRACH. Combined natural and forced-convection laminar flow and heat transfer of fluids with and without heat sources in channels with linearly varying wall temperatures. NACA TN 3141 (1954).
5. S. OSTRACH. Laminar natural-convection flow and heat transfer of fluids with and without heat sources in channels with constant wall temperatures. NACA TN 2863 (1952).

6. L. N. TAO. On combined free and forced convection in channels. *J. Heat Transfer* **82**, 233–238 (1960).
7. T. S. LAUBER and A. U. WELCH. Natural convection heat transfer between vertical flat plates with uniform heat flux. Proceedings of Third International Heat Transfer Conference. Chicago. Illinois. pp. 126–131 (1966).
8. L. P. DAVIS and J. J. PERONA. Development of free convection flow of a gas in a heated vertical open tube. *Int. J. Heat Mass Transfer* **14**. 889–903 (1971).
9. W. AUNG. Fully developed laminar free convection between vertical plates heated asymmetrically, *Int. J. Heat Mass Transfer* **15**, 1577–1580 (1972).
10. V. SERNAS and L. S. FLETCHER. A schlieren interferometer method for heat transfer studies. *J. Heat Transfer* **92**, 202–204 (1970).
11. V. SERNAS. L. S. FLETCHER and J. A. JONES. An interferometric heat flux measuring device. ISA Paper 618–70. Proceedings of the 25th Annual ISA Conference. Philadelphia, Pennsylvania (October 1970).
12. V. SERNAS and C. R. CARLSON. Density gradient measurements with a wollaston prism schlieren interferometer. Rutgers University. Department of Mechanical and Aerospace Engineering. Report RU-TR 129-MAE-F (April 1970).
13. W. AUNG and R. O'REGAN. Precise measurement of heat transfer using holographic interferometry. *Rev. Scient. Instrum.* **42**. 1755–1759 (1971).
14. J. KIELBASA and J. RYSZ. Measurement of low air flow velocities by a hot wire constant temperature anemometer. *Bull. de l'Academie Polonaise des Sciences. Serie des Sciences Techniques* **XVI**. 147–152 (1968).
15. E. M. SPARROW and J. L. GREGG. Laminary free convection from a vertical plate with uniform surface heat flux, *Trans. Am. Soc. Mech. Engrs* **78**, 435–440 (1956).

CONVECTION LIBRE LAMINAIRE SE DEVELOPPANT ENTRE DES PLAQUES PLANES VERTICALES AVEC CHAUFFAGE ASYMETRIQUE

Résumé—On présente une étude numérique et expérimentale du transfert thermique par convection naturelle laminaire se développant dans des canaux entre plans parallèles verticaux avec chauffage asymétrique. On considère les conditions limites de flux thermiques uniformes à la paroi (UHF) et de température uniforme à la paroi (UWT). Des solutions d'écoulement se développant sont obtenues pour l'air à des rapports différents de flux thermiques pariétaux et de différences de température pariétales (supérieures à la température du fluide à l'entrée du canal). Les solutions numériques approchent asymptotiquement la solution analytique pour un écoulement entièrement développé. Les résultats indiquent que pour UHF, la différence entre les températures maximales sur les deux parois diminue jusqu' à ce que l'écoulement soit entièrement établi. Pour UWT le nombre de Nusselt caractérisant le transfert thermique total au fluide est lié au nombre de Rayleigh par une courbe universelle pour tous les rapports de différences de température pariétale, donnant les nombres de Nusselt et Rayleigh correspondants.

AUSBILDUNG LAMINARER FREIER KONVEKTION ZWISCHEN VERTIKALEN, EBENEN PLATTEN MIT ASYMMETRISCHER HEIZUNG.

Zusammenfassung—Eine numerische und experimentelle Untersuchung der Wärmeübertragung bei sich ausbildender laminarer freier Konvektion in Kanälen zwischen vertikalen, parallelen Platten mit asymmetrischer Heizung wird beschrieben. Als thermische Grenzschichtbedingungen werden betrachtet: konstanter Wärmefluss an der Wand und konstante Wandtemperatur. Lösungen für die sich ausbildende Strömung werden für Luft bei verschiedenen Verhältnissen von Wärmefluss an der Wand zu Wandtemperaturdifferenz (oberhalb der Temperatur des Fluids am Kanaleingang) erhalten.

Es wird gezeigt, dass sich die numerische Lösung asymptotisch der geschlossenen Lösung für voll ausgebildete Strömung nähert. Die vorgelegten Ergebnisse zeigen, dass sich bei konstantem Wärmefluss die Differenz zwischen den maximalen Temperaturen der zwei Wände verringert, wenn voll ausgebildete Strömung erreicht wird.

Für konstante Wandtemperatur findet man, dass die Beziehung zwischen Nusselt-Zahl—sie charakterisiert hier den totalen Wärmeübergang auf das Fluid—und der Rayleigh-Zahl für alle Verhältnisse der Wandtemperatur in guter Näherung durch eine universelle Kurve dargestellt werden kann. Vorausgesetzt wird, dass dies Nusselt-Zahlen und die Rayleigh-Zahlen in geeigneter Weise definiert werden.

РАЗВИВАЮЩАЯСЯ ЛАМИНАРНАЯ СВОБОДНАЯ КОНВЕКЦИЯ МЕЖДУ ВЕРТИКАЛЬНЫМИ ПЛОСКИМИ ПЛАСТИНАМИ ПРИ АСИММЕТРИЧНОМ НАГРЕВЕ

Аннотация—Представлены численное и экспериментальное исследование переноса тепла при развивающейся ламинарной свободной конвекции в вертикальных каналах с параллельными стенками при асимметричном нагреве. В качестве граничных условий принимались постоянный тепловой поток на стенке и постоянная температура стенки. Получены решения для развивающегося потока воздуха при различных отношениях

тепловых потоков на стенке и разности температур стенки (выше температуры жидкости на входе в канал). Показано, что численные решения асимптотически приближаются к точному решению для полностью развитого потока.

Представленные результаты показывают, что при однородных тепловых потоках на стенке различие между максимальными значениями температур на обеих стенках уменьшается по мере того, как достигается полное развитие потока.

При постоянной температуре стенок число Нуссельта, характеризующее суммарный теплоперенос, при всех исследованных разностях температур стенок связано с числом Релея универсальным соотношением при условии, если числа Нуссельта и Релея определены соответствующим образом.